Biosensors for Characterizing the Dynamics of Rho Family GTPases in Living Cells

Louis Hodgson,[1] Feimo Shen,[2] and Klaus Hahn[2]

[1]Gruss-Lipper Biophotonics Center, Department of Anatomy and Structural Biology, Albert Einstein College of Medicine of Yeshiva University, Bronx, New York
[2]University of North Carolina at Chapel Hill, Chapel Hill, North Carolina

ABSTRACT

The biosensors developed in the authors' laboratory have been based on different designs, each imparting specific strengths and weaknesses. Here we describe detailed protocols for the application of three biosensors exemplifying different designs—first, a design in which an environmentally sensitive dye is used to report the activation of endogenous Cdc42, followed by two biosensors based on FRET, one using intramolecular and the other intermolecular FRET. The design differences lead to the need for different approaches in imaging and image analysis. *Curr. Protoc. Cell Biol.* 46:14.11.1-14.11.26.
© 2010 by John Wiley & Sons, Inc.

Keywords: biosensors • Rho family GTPases • FRET • live cell imaging

INTRODUCTION

In this unit, we describe detailed protocols for the application of three biosensors developed in our laboratory, exemplifying different designs with specific strengths and weaknesses. The first biosensor described represents a design in which an environmentally sensitive dye is used to report the activation of endogenous Cdc42. Also described are two biosensors based on fluorescence resonance energy transfer (FRET; also see *UNIT 17.1*), one using intramolecular and the other intermolecular FRET. The design differences lead to the need for different approaches in imaging and image analysis.

Figure 14.11.1 shows the design of the three biosensors. MeroCBD (Fig. 14.11.1A) is a sensor for Cdc42 activation in which a fragment of Wiskott-Aldrich Syndrome protein that binds only to active Cdc42 is derivatized with an environmentally sensitive dye (Nalbant et al., 2004). In living cells, the dye undergoes a fluorescence change when the biosensor binds to endogenous, untagged Cdc42. This design is advantageous for several reasons: Cdc42 is not tagged with a fluorophore or other biosensor component, expression of exogenous Cdc42 is not needed, and the signal is substantially brighter than FRET because a bright dye is directly excited, rather than indirectly as in FRET. The major disadvantage is that the biosensor is not genetically encoded, so must be loaded in the cells, e.g., via microinjection or electroporation.

The FRET biosensor for RhoA (Pertz et al., 2006) is shown in Figure 14.11.1B. A fragment of Rhotekin is attached directly to RhoA, and fluorescent proteins undergoing FRET are built into the chain connecting the RhoA and Rhotekin fragment. The C terminus of the RhoA is purposely left free of fluorescent protein or other modifications, to maintain intact the regulation of RhoA by GDI. Unlike the Cdc42 biosensor, this biosensor is completely genetically encoded, greatly simplifying loading into cells.

Finally, the biosensor for Rac1 is shown in Figure 14.11.1C. Named Rac1 FLAIR, it is a modification of a design originally published using a covalently attached fluorescent dye

Current Protocols in Cell Biology 14.11.1-14.11.26, March 2010
Published online March 2010 in Wiley Interscience (www.interscience.wiley.com).
DOI: 10.1002/0471143030.cb1411s46
Copyright © 2010 John Wiley & Sons, Inc.

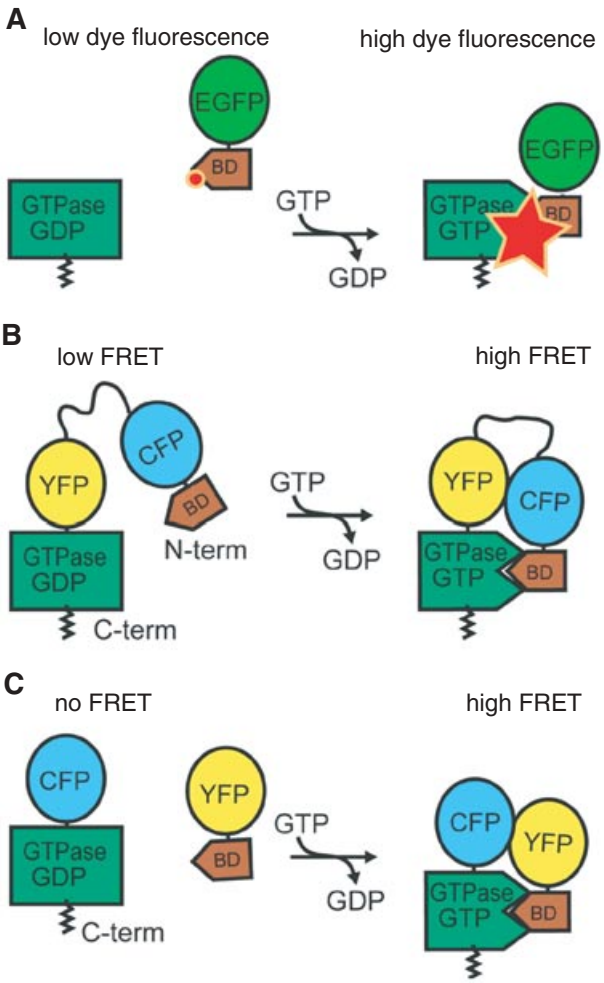

Figure 14.11.1 Fluorescent biosensor designs. (**A**) MeroCBD, biosensor of endogenous Cdc42 activation. Here, a fragment of Wiskott-Aldrich syndrome protein (WASP) that binds only to activated Cdc42 is covalently derivatized with an environmentally sensitive dye. When the WASP fragment encounters and binds to activated Cdc42, the solvation of the dye by water is reduced, leading to a fluorescence change. Advantages of this design include the ability to study endogenous protein, and enhanced sensitivity due to direct excitation of a bright, long-wavelength dye (as opposed to indirect excitation via FRET). The disadvantage is the need for microinjection, electroporation, or some other means to load the covalently tagged protein biosensor into cells. (**B**) RhoA biosensor. Here a fragment of Rhotekin that binds only to activated RhoA is attached to RhoA as part of the same protein chain. Two different fluorescent proteins undergoing FRET are in the chain between RhoA and the Rhotekin fragment, such that binding of the fragment to activated RhoA alters the distance and/or orientation between the fluorescent proteins, affecting FRET. This biosensor is fully genetically encoded, greatly simplifying loading into the cell. Because the Rhotekin fragment is attached to the RhoA, image processing is simplified relative to the dual-chain sensor shown in (C) (see text). (**C**) Rac1 FLAIR, biosensor of Rac1 activation. This design is similar to that of the RhoA biosensor, but here the PAK fragment used to bind activated Rac1 is not part of the same chain as the Rac1. The use of a dual-chain, intermolecular FRET design enhances sensitivity because, unlike the single-chain design, there is no FRET when the biosensor is in the off state. Additional image processing (bleed-through correction) is required because the biosensor components can distribute differently throughout the cell. For color figure go to *http://www.currentprotocols.com/protocol/cb1411*.

for FRET (Kraynov et al., 2000). In the modification described here, the dye has been replaced with a fluorescent protein, rendering the biosensor fully genetically encoded (Machacek et al., 2009). A fragment of p21-activated kinase (PAK) is used to bind specifically to activated Rac1. The main difference between this design and that of the RhoA biosensor is that the PAK fragment is not attached to Rac1. Rac1 FLAIR is an intermolecular FRET biosensor, frequently referred to as a dual-chain sensor.

NOTE: All solutions and equipment coming into contact with cells must be sterile, and proper aseptic technique should be used accordingly.

NOTE: All culture incubations should be performed in a humidified 37°C, 5% CO_2 incubator unless otherwise specified.

PRODUCTION AND USE OF meroCBD, DYE-BASED BIOSENSOR FOR CDC42

BASIC PROTOCOL 1

As discussed above, the meroCBD biosensor for Cdc42 activation is based on a fragment of WASP (the Cdc42 binding domain, CBD) that binds only to activated Cdc42. This fragment is covalently coupled to a solvent-sensitive dye that increases in fluorescence intensity when the CBD interacts with endogenous, activated Cdc42 (Toutchkine et al., 2003, 2007a,b). Because the dye responds to Cdc42 binding with an intensity change, rather than with a shift in λ_{max}, it is useful to attach a second fluorophore to the biosensor for ratio imaging.

CBD-EGFP is expressed in the form of a C-terminal 6× His fusion from the prokaryotic expression vector pET23. This vector has a strong T7 promoter, and is designed to work with BL21(DE3) strains of *E.coli* (Stratagene). It was determined experimentally that the highest levels of expression are observed when a plain T7 promoter (not T7*lac*) is used in combination with a BL21(DE3) strain, and not BL21(DE3)pLysS. The BL21(DE3) strain is more leaky, but this is not of great consequence, as CBD-EGFP shows no appreciable toxicity. The protein is best induced and expressed at room temperature (26°C), which increases the proportion of correctly folded, soluble CBD-EGFP.

Materials

Transformation-competent BL21(DE3) *E. coli* (e.g., Stratagene)
pET23-CBD-EGFP (Addgene)
LB medium and plates (*APPENDIX 2A*) containing 100 μg/ml carbenicillin
1 M IPTG (in water), store at −20°C
Lysis buffer (see recipe)
Talon resin (Co^{2+} affinity, Clontech)
Lysis buffer (see recipe but omit 2-ME and PMSF) containing 5 mM and 150 mM imidazole
50 mM Tris·Cl, pH 7.5 to 8.0 (*APPENDIX 2A*)
50 mM sodium phosphate buffer, pH 7.5 (*APPENDIX 2A*)
Storage buffer (see recipe)

2000-ml Erlenmeyer flask
Incubator with shaker
250-ml centrifuge bottles
Beckman centrifuge with JA-10 and JA-20 rotors (or equivalent)
50-ml conical polypropylene centrifuge tubes (Falcon)
Centrifuge with swinging-bucket rotor
End-over-end rotator
Ultrafree Centrifugal Filtration Device (MWCO, 5000; Fisher Scientific, cat. no. UFV5BCC25)
Slide-A-Lyzer cassettes (MWCO 3500; Pierce)

Additional reagents and equipment for transformation of bacteria and other basic molecular biological techniques (e.g., Sambrook et al., 1989; Ausubel et al., 2009), SDS-PAGE (*UNIT 6.1*), and dialysis (*APPENDIX 3H*)

NOTE: Use the buffers suggested in this unit. Apparently small changes have proven to greatly reduce yield.

Day 1: Transform the bacteria

1. Transform competent BL21(DE3) *E. coli* cells with pET23-CBD-EGFP according to standard protocols (Sambrook et al., 1989; Ausubel et al., 2009), and plate on LB plates containing 100 μg/ml carbenicillin.

   The 200-μl transformation volume should be split over two plates.

   The bacterial strain is critical. BL21(DE3) are recommended. Do not use BL21(DE3)pLysS.

2. Incubate plates at 37°C overnight.

Day 2: Grow and induce the transformed bacteria

3. Inoculate 500 ml of LB liquid medium containing 100 μg/ml carbenicillin with the colonies from the plates by adding 5 ml of medium to each plate and resuspending the cells into the medium, then transferring the cell suspension into 500 ml LB medium/carbenicillin (in a separate 2000-ml Erlenmeyer flask for each plate) and growing at 37°C with shaking at 225 rpm, to an OD_{600} of 0.8 to 0.9.

4. Briefly chill the culture on ice to 26°C and put back in the shaking incubator, with temperature reduced to 26°C.

5. Add IPTG (1 M stock in water, kept at –20°C) to a final concentration of 0.2 mM, and allow the cultures to grow for another 6 hr at 26°C at 225 rpm.

   IPTG concentrations of 0.2 to 0.5 mM have been used successfully.

6. Transfer cells to 250-ml centrifuge bottles. Collect cells by centrifuging 10 min at 6000 × *g*, 4°C, and store as a pellet at –20°C until use.

   Approximately 2.5 to 3 g of cells is usually obtained from each liter of culture.

Day 3: Prepare the lysate

7. Resuspend cells (~3 g) in 35 ml of lysis buffer in a 50-ml conical tube and lyse by sonication with a probe sonicator (four pulses, 30 sec each, on ice with 1-min intervals).

8. Centrifuge the lysates 30 min at 20,000 × *g* (13,000 rpm in a JA-20 rotor), 4°C, and carefully transfer the supernatant containing CBD-EGFP into a 50-ml conical polypropylene centrifuge tube.

Day 3: Prepare the resin

9. While the lysates are being centrifuged, transfer 2 ml of Talon resin (dry volume) into a 50-ml conical polypropylene centrifuge tube and centrifuge 3 min at 700 × *g*, 24°C, in a centrifuge with a swinging-bucket rotor. Remove supernatant.

   Do not use Ni-NTA resin.

   A ratio of 2 ml resin per 3 g cell pellet is recommended.

10. Wash Talon resin twice, each time by adding 10 volumes of lysis buffer without 2-mercaptoethanol or PMSF centrifuging 3 min at 700 × *g*, 24°C, and removing the supernatant.

Day 3: Bind the CBD-EGFP to the resin

11. Add the cell lysate to the washed Talon resin in the 50-ml tube, wrap in foil, and invert gently using an end-over-end rotator at room temperature for 40 min to 1 hr.

    The tube is wrapped in foil to avoid unnecessary exposure of EGFP to light.

12. Separate the unbound material by centrifuging 3 min at 700 × *g*, 24°C, in a centrifuge with a swinging-bucket rotor.

13. Remove and save the supernatant (unbound fraction) for SDS-PAGE analysis (*UNIT 6.1*).

    If a large portion of unbound material is present in this fraction, consider increasing the Talon resin volume by preparing two tubes of 2 ml resin and splitting the lysates into two tubes during the binding reaction.

14. Wash the resin twice, each time by adding 20 ml fresh lysis buffer without PMSF or 2-mercaptoethanol, rotating for 5 min at room temperature on an end-over-end rotator, then centrifuging as in step 12 and removing the supernatant.

15. Perform the final resin wash with 10 volumes of lysis buffer containing 5 mM imidazole (no PMSF or 2-ME).

    It is important to prepare a fresh 5 ml of 1 M imidazole stock solution in the same buffer. Always prepare the stock imidazole solution fresh.

Day 3: Elute the resin

16. Perform the elution by adding 5 ml of lysis buffer (no PMSF or 2-ME) containing 150 mM imidazole to the resin and then rotating using an end-over-end rotator for 5 min. Pellet the resin again by centrifugation for 3 min at 700 × *g*, 24°C.

17. Remove the supernatant and save (eluted fraction).

18. Concentrate the resulting 5-ml eluate with a centrifugal concentrator by centrifugation at 4°C according to the manufacturer's instructions. Check the concentration process every 20 min to ensure proper filtration.

    Do not over-concentrate; optimal final concentration should be ∼120 μM.

19. Measure the concentration of CBD-EGFP by taking a small aliquot (5 to 10 μl) and diluting 1:10 into 50 mM Tris·Cl, pH 7.5 to 8.0.

20. Determine protein concentration using the absorption at 280 with an extinction coefficient of 28,260 (cm^{-1} M^{-1}), and Equation 14.11.1:

$$[\text{CBD}-\text{EGFP}](\text{in mol/liter}) = \frac{\text{OD}_{280} \times \text{dilution factor}}{28,260}$$

Equation 14.11.1

    On average, 10 to 20 mg of CBD-EGFP is obtained per liter culture.

21a. *If dye-labeling is to be performed the following day:* Dialyze a part of the concentrated protein overnight against 2 liters of 50 mM sodium phosphate buffer, pH 7.5, at 4°C (*APPENDIX 3H*).

    Slide-A-Lyzer cassettes (Pierce) with a molecular weight cut-off of 3,500 Da can be conveniently used.

21b. *For long-term storage:* Dialyze the protein overnight against 2 liters of storage buffer at 4°C (*APPENDIX 3H*), and freeze at −80°C.

    Freezing at −80°C appears to be better than flash freezing for this protein.

SUPPORT PROTOCOL

LABELING CBD-EGFP WITH REACTIVE FLUOROPHORE

Dyes are available from the Hahn lab and should be commercially available soon. Solvent-sensitive dyes other than those that have been used to date should also respond to Cdc42 binding.

Materials

Dye: ISO-IAA (Toutchkine et al., 2003, 2007a,b)
Dimethylsulfoxide (DMSO)
CBD-EGFP (Basic Protocol 1)
2-mercaptoethanol (2-ME)
50 mM sodium phosphate buffer, pH 7.5 (*APPENDIX 2A*)
12% SDS-PAGE gel (*UNIT 6.1*)
50 mM Tris·Cl, pH 8.0 (*APPENDIX 2A*)

Spectrophotometer
2-ml microcentrifuge tubes
End-over-end rotator
0.5 cm × 6 to 8 cm column packed with Sephadex G15 gel-filtration resin (GE Healthcare)

Additional reagents and equipment for SDS-PAGE (*UNIT 6.1*) and spectrophotometric determination of protein concentration (*APPENDIX 3B*)

Prepare dye stock solution

1. Prepare a fresh solution of dye, ISO-IAA, in pure DMSO by adding ~1 mg of dye into 30 to 40 µl DMSO.

   Once dissolved in DMSO, the dye should be used immediately.

2. Determine the exact concentration of the dye spectrophotometrically at 593 nm by diluting a small aliquot of the DMSO solution 1:5,000 to 1:10,000 in additional DMSO. For ISO-IAA, assume an extinction coefficient in DMSO at maximum absorption (593 nm) of 135,000 (cm^{-1} M^{-1}):

$$[\text{ISO}-\text{IAA}](\text{in mol/liter}) = \frac{\text{OD}_{593} \times \text{dilution factor}}{135,000}$$

Equation 14.11.2

   The authors routinely obtain concentrations of 30 to 40 mM for the DMSO stock solution.

Label the protein

3. Transfer a 300-µl aliquot of fresh CBD-EGFP protein into a 2-ml microcentrifuge tube wrapped in foil to protect from light.

   For attachment of the dyes to cysteine, CBD-EGFP needs to be in 50 mM sodium phosphate buffer, pH 7.5 (APPENDIX 2A), at a protein concentration of 200 µM.

4. Add the dye to the CBD-EGFP solution in two to three aliquots to bring the final dye-to-protein molar ratio in the reaction to 6:1.

   The molecular weight of the ISO-IAA is ~1300 Da, and the molecular weight of the CBD-EGFP is ~36.5 kDa.

   This ratio can be further optimized depending on the reactivity of the dye if different dyes are used. We suggest 6:1 as a useful starting point.

Using higher dye-to-CBD-EGFP ratios (e. g. 10:1 or 15:1) in the reaction mixture can produce excessive amounts of precipitated material and "over-labeling" (dye to protein ratio in the purified covalent adduct >1.0 due to labeling of the exposed cysteine in EGFP). EGFP mutants lacking surface cysteines can be used to ameliorate this problem. The optimal dye-to-protein ratio to use in the reaction mixture depends on the reactivity of the dye, so it can vary for different dyes, or dyes from different sources/batches.

5. Vortex the protein/dye mix once briefly at the highest setting, immediately after addition of the dye stock solution.

   Avoid excess mixing as this may denature the protein.

6. Wrap the tube containing the reaction mixture in foil and gently rotate on an end-over-end rotator at room temperature for exactly 1 hr.

   Here, the time is critical; longer reaction times result in over-labeling of the protein.

7. After the reaction is complete, add 1 to 5 μl of 2–ME to stop the reaction, and incubate the tube 5 to 10 min at room temperature on the end-over-end rotator.

8. Microcentrifuge the tube 2 min at 13,000 × *g*, room temperature, to pellet insoluble material.

9. Load the supernatant on a 0.5 cm × 6 to 8 cm G15 gel-filtration column to separate the conjugate from free dye. Equilibrate and run this column in 50 mM NaH_2PO_4 buffer at pH 7.5. Collect fractions of ∼200 μl each.

   The first colored band to elute contains the dye-labeled CBD-EGFP (meroCBD).

Analyze the labeled protein

10. Analyze an aliquot (3 to 5 μl) of each fraction on a 12% SDS-PAGE gel (*UNIT 6.1*) to confirm the presence and purity of the meroCBD. Visualize the gel with fluorescent illumination using a UV transilluminator or a hand-held UV lamp.

    Fluorescence visualization of the gel ensures labeling with the dye, and can reveal a band of free dye running at much lower molecular weight, often near marker dyes used in the electrophoresis sample.

11. To evaluate the success of the procedure, and generation of an optimal biosensor, determine the dye/protein ratio once the biosensor has been freed from unattached dye.

Determine protein concentration

It is also important to know the protein concentration to optimize later microinjection in living cells.

12. Determine an approximate protein concentration rapidly by taking an absorbance spectrum of the conjugate solution. Dilute a small aliquot (5 to 10 μl) in 50 mM Tris·Cl, pH 7.5 to 8.0, and use OD_{280} and Equation 14.11.1 above (also see *APPENDIX 3B*).

    Importantly, the protein absorbance at 280 overlaps dye absorbance.

13. Correct this overlapping absorbance by subtracting, from the OD_{280}, a fraction of the dye's absorbance at its maximum (∼593 nm); however, this is variable due to the solvent sensitivity of the dye. For a more accurate measure, compare a sample of the meroCBD (dye-labeled CBD-EGFP) to unlabeled CBD-EGFP by running them on the same gel, using different known concentrations of the unlabeled protein.

    Colorimetric assays, limited to those whose readouts do not overlap dye absorbance, have proven less reliable in our hands.

Determine the dye concentration

14. Determine the dye concentration by taking an absorbance spectrum of meroCBD. Dilute 5 to 10 μl of meroCBD in 100 μl DMSO.

    DMSO as a solvent will denature and overwhelm the effect of the protein or buffer on the dye's absorbance, resulting in a consistent dye extinction coefficient.

15. Use the OD at the dye absorbance maximum of 593 nm to calculate the dye concentration, using Equation 14.11.2 above.

BASIC PROTOCOL 2

IMAGING meroCBD IN LIVING CELLS

The authors of this unit routinely microinject cells on coverslips and image meroCBD following 30 min of recovery time in a tissue culture incubator. MeroCBD can produce puncta (possibly autophagy) after 2 to 3 hr in some cells, in which case the timing between microinjection and observation must be carefully controlled.

Cells are observed in a live-cell chamber atop an inverted epifluorescence microscope outfitted with an Hg arc-lamp light source. When imaging with a single camera, excitation and emission filter wheels can be used to alternately illuminate the dye and EGFP to obtain a ratiometric image set at every time point during the time-lapse experiment. If two cameras are available, two-camera modules such as those available from Olympus (U-DPCAD module), Technical Video (Technical Video Inc.), or Optical Insights (Dual-Cam) can be used to acquire two images simultaneously using a dual band-pass excitation filter. Since the dye and EGFP will have different brightnesses, band-pass filters can be designed to pass different amounts of excitation light at each wavelength through the dual band-pass filter.

When meroCBD is made using I-SO type fluorophores (Toutchkine et al., 2003, 2007a,b), including the new dyes we currently employ (Dyes 53 and 87; manuscript in preparation), EGFP bleed-through into the dye channel is practically zero. This is made possible by using relatively narrow excitation and emission band-pass filters. We use a customized multiband-pass dichroic mirror (Fig. 14.11.2) and the following excitation and emission filters: HQ470/40 and HQ525/50 for EGFP; HQ580/30 and HQ630/40 for dye (Chroma Technology).

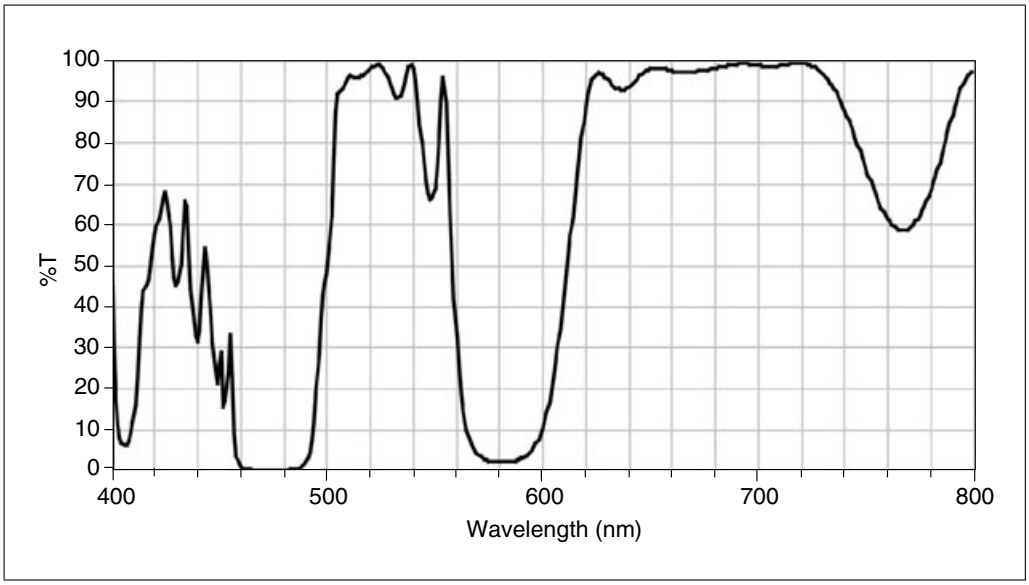

Figure 14.11.2 Transmittance spectra for the "Scripps Custom" dichroic mirror (Chroma Technology, lot no. 511111886).

The interval between images will vary depending on the images. We routinely acquire images at 10-sec to 1-min time intervals using 2 × 2 binning on a full-field 1.3k-by-1.0k cooled CCD camera. Importantly, the excitation light from the 100 W Hg arc lamp source is too bright, so it is routinely reduced using neutral-density filters for 4% to 10% transmittance (ND 1.4 to 1.0). The integration (exposure) time on a CCD camera depends on the quantum efficiency of the CCD and the noise characteristics of the camera. The dye exposure is usually 0.5× to 0.3× as long as the EGFP exposure. Dye exposure times may be reduced with some cameras; many current cameras, including those we use, are less efficient at the red wavelengths of the dyes. Users should fine-tune the exposure times depending on their optics and camera setup. Ideally, the integrated average intensity from both fluorescence channels should be similar, to maximize the dynamic range of the data. Cameras with 12-bit depth have an intensity range from 0 to 4096; we routinely fill ∼3000 of this dynamic range in a single field of view. We carefully monitor the pixel intensities near the cell periphery where the signals are usually low, aiming for approximately 100 to 200 over the background values. This translates to 2 to 3 in signal-to-noise ratio at the darkest regions.

Because different wavelengths are used to image EGFP and dye, many objectives (even apochromatic objectives) will focus on slightly different planes within the specimen. The *z*-axis difference between these two focal planes needs to be calibrated, and the objective slightly offset between the two images. We use a *z*-axis position control on our microscope to accomplish this. Typically, the *z*-distance offset is determined by focusing on the same small object at different wavelengths, using image-based autofocus (Shen et al., 2006, 2008) followed by manual fine adjustment. A script is written to execute the shifts in *z* for each color acquired during an automated time-lapse sequence. Moving the objective turret back and forth in different directions to account for these *z* offsets will not give reproducible results, due to hysteresis in the focus drive mechanism. Therefore, it is better to acquire different colors so that the objective always changes *z* position in one direction. Alternatively, a linear-encoder feedback or piezo-stage system can be installed for precise *z* positioning, to eliminate the hysteresis problem. It is important to always set the search range for autofocus to be more than twice as large as the total motions programmed in for *z* focus offset.

EXPRESSING THE RhoA SINGLE-CHAIN BIOSENSOR

BASIC PROTOCOL 3

The genetically encoded biosensor for RhoA consists of (N-terminus to the C-terminus) a small RhoA-binding domain (RBD) derived from the RhoA effector Rhotekin, ECFP, an unstructured linker of optimized length, pH-insensitive Citrine-YFP, and a full-length RhoA (Fig. 14.11.1B). Three different expression constructs for this single-chain biosensor have been developed, all available from the nonprofit distributor Addgene (*http://www.addgene.org*):

1. pTriEX mammalian expression and cloning vector (pTriEX-RhoA/amp resistance).

2. pBabe retroviral expression vector (pBabe-RhoA/amp resistance).

3. pBabe-sin-tet-CMV-puro retroviral vector for Tet-On/Off system (pBabe-sin-tet-CMV-puro-RhoA/amp resistance).

The pTriEX backbone is used for the cloning of the biosensor, and the complete biosensor cDNA can be cut out as a cassette by digesting with *Nco*I/*Xho*I. *Nco*I encodes the start codon, and *Xho*I is placed in-frame immediately following the stop codon after the RhoA GTPase. The pTriEX version of the biosensor allows overexpression in mammalian cells driven by the CMV promoter.

One must beware of the potential toxicity of GTPases upon overexpression (Pertz et al., 2006) and the importance of the relative intracellular concentrations of GTPases and upstream regulators in cells (Michaelson et al., 2001; Del Pozo et al., 2002). We have addressed these issues by using retroviral transduction to stably incorporate low copy numbers of the biosensor DNA using the pBabe expression system (Pertz et al., 2006). Transduced cells are sorted flow cytometrically to obtain low to medium expressors only, so that the biosensor expression level is comparable to endogenous GTPase. We have shown that competition with endogenous effectors of the GTPase is not a significant problem at appropriate biosensor concentrations (Pertz et al., 2006).

In order to address the toxicity of overexpressed biosensor, a tetracycline-inducible retroviral construct based on a pBabe-sin-tet-CMV-puro backbone is used.

Materials

Tet-off stable MEF/3T3 cell system (Clontech)
MEF/3T3 cells transduced with the appropriate construct
10 mg/ml doxycycline stock solution
10 mg/ml puromycin stock solution

10-cm tissue culture dishes
Coverslips coated with fibronectin: immerse glass coverslips 30 to 60 min in 10 μg/ml fibronectin (e.g., Sigma), then rinse three times with PBS (*APPENDIX 2A*) and leave immersed in PBS until use

Additional reagents and equipment for cell culture techniques including trypsinization (*UNIT 1.1*), flow cytometric cell sorting (Robinson et al., 2009), and imaging the RhoA biosensor (Basic Protocol 4)

1. Using the tet-off stable MEF/3T3 cell system (Clontech), repress infected cells using 1 μg/ml doxycycline.

   Refer to user's guide for Clontech tet-off stable MEF/3T3 cell system for this and the following step.

2. Select cells with puromycin up to 10 μg/ml, increasing the puromycin concentration gradually following the infection (2 μg/ml increase per each successive selection cycle).

   "Selection cycle" means that the cells have tolerated that particular puromycin concentration.

3. At the end of selection, induce cells for biosensor expression by removal of doxycycline and replating cells at a sparse concentration (1×10^4 cells per 10-cm tissue culture dish) for 48 hr.

4. Sort cells flow cytometrically (Robinson et al., 2009) to produce nearly 100% biosensor-positive cells. Sort for CFP and YFP using two-color system.

5. Repress the cells again by application of 1 μg/ml doxycycline.

   We routinely maintain repressed cells in 1 μg/ml doxycycline under standard tissue culture conditions.

6. For the induction of the biosensor prior to experiments, detach the cells by brief trypsinization (*UNIT 1.1*) and centrifuge 5 min at $300 \times g$, 24°C. Carefully remove the supernatant and resuspend the cells in medium without doxycycline.

7. Plate the cells sparsely (1×10^4 cells per 10-cm tissue culture dish) without doxycycline and incubate for 48 hr prior to the experiments.

8. At a time point 24 hr after induction (i.e., the plating in step 7), check the cells for fluorescence. Continue incubating the cells under doxycycline-free conditions for an additional 24 hr prior to the assay.

   The total of 48 hr after removal of doxycycline ensures that overexpressors die and only cells with a sustainable expression level survive for the experiment.

9. On the day of the experiment, detach the cells with a brief trypsinization (*UNIT 1.1*).

10. Replate the cells on coverslips coated with fibronectin on the morning of the experiment and allow to adhere for 5 hr prior to imaging (see Basic Protocol 4).

IMAGING THE RhoA BIOSENSOR

BASIC PROTOCOL 4

Imaging is performed with the cells in Ham's F-12K medium without phenol red (see recipe in Reagents and Solutions), supplemented with 2% fetal bovine serum (FBS). For a single-chain design, it is sufficient to simply take a ratio of the FRET emission over the donor emission (Pertz et al., 2006). The two fluorophores will bleach at different rates, so bleaching corrections may be required to counter a bias in the signal over time. Such photobleach corrections are covered in detail elsewhere (Hodgson et al., 2006). Correcting for bleed-through (discussed in Basic Protocol 7) is not required for single-chain biosensors, but can be used to improve dynamic range when the biosensor is bright enough to permit this additional image processing.

This biosensor design preserves upstream regulatory interactions with molecules requiring a free C terminus, such as GDI. While this is an advantage in accurately reflecting cell physiology, it requires that one maintain low, near-endogenous levels of biosensor to minimize perturbation of normal cell physiology. At these low biosensor levels one must be careful to maximize light collection. It is not possible to compensate for low biosensor concentrations simply by increasing irradiation, as this bleaches the biosensor and increases phototoxicity. We routinely use an oil-immersion 40× Olympus UIS2 DIC objective lens with a numerical aperture of 1.3, together with 2 × 2 binning on our cooled CCD camera. We find that using 60× or higher magnification objectives cuts down greatly on light collection while increasing the photobleach rate. The signal intensity scales to the 4th power of the numerical aperture and to the inverse square of the magnification. Therefore, switching from a 1.3 NA 40× DIC objective lens to a 1.42 NA 60× DIC objective lens will result in an ∼37% decrease in signal intensity. It is important to use DIC rather than phase-contrast objective lenses, as the phase objective contains a phase annulus that substantially reduces light transmittance. Neutral-density filters of 0.6 to 1.0 (25% transmittance to 10% transmittance) are used to cut the brightness of the excitation light. It is better to use longer exposure with dimmer excitation rather than shorter, more intense irradiation; this reduces both photobleaching and phototoxicity. We routinely use methods to remove oxygen from the medium to further decrease photobleaching and phototoxicity, such as including the oxygen scavenger OxyFluor (Oxyrase, Inc.), including antioxidants such as vitamin C at 1 mM concentration, and purging the assay medium with argon gas.

The authors of this unit currently use a Roper Photometrics CoolSnapESII camera (*http://www.roperscientific.com/*), which is a Sony ICX285-based interline transfer cooled CCD camera, cooled to 0°C. This camera can be obtained with $<6e^-$ read noise, and $0.1e^-$/pixel/second dark current. The quantum efficiency of the chip is ∼60% for 450- to 625-nm light, and it has a small pixel size (6.45 × 6.45 μm) for good spatial resolution. We routinely use 2 by 2 binning and expose 800 msec for CFP and 400 msec for FRET, with a 10% transmittance neutral-density filter in the excitation light path. These conditions usually result in gray values filling ∼75% of the full 12-bit

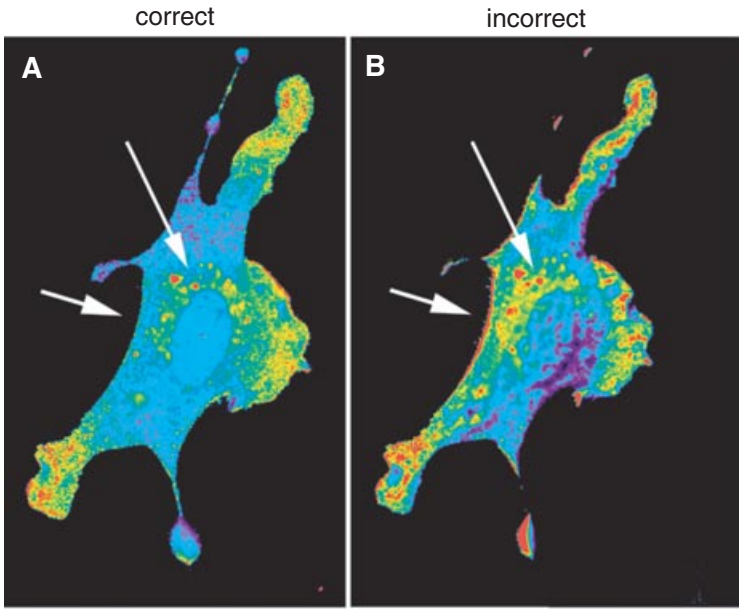

Figure 14.11.3 *x-y* translational image registration artifacts generate features on ratio images. In panel (**A**), a correctly registered ratio image of MeroCBD is shown. Panel (**B**) shows the ratio image from the same cell without registration. In the latter case, the dye image was misaligned by −5 pixels in both x and y directions. The white arrows in both figures point to regions where misalignment produces edge artifacts and other artifactual features. In (B), a lower-ratio rim can be seen on one side of the nucleus, and a higher ratio on the opposite side. Similarly, edge artifacts appear as higher ratio on predominantly one side of the cell, with an artifactually low ratio on the opposite side. For color figure go to *http://www.currentprotocols.com/protocol/cb1411*.

range of camera digitization. We do not recommend the current generation of on-chip amplification-gain CCD (EM-CCD) cameras for biosensor imaging. While these cameras can capture images under extremely dark illumination conditions, the gain circuitry introduces large amount of stochastic noise, which is problematic for ratiometric imaging (Fig. 14.11.3). When mathematical operations are performed on raw images, the stochastic noise adds greatly to the total noise levels in the resulting ratio image. While there are techniques available for signal restoration from acquisition with EM-CCD and other noisy approaches (Wang, 2007a,b), we have found conventional cooled CCD cameras to be sufficient. Other viable options may include back-thinned, back-illuminated cooled CCD cameras with high quantum efficiency. These cameras offer ultra-high quantum efficiency (>90%), but the pixel size is usually large (16 × 16 μm), reducing spatial resolution.

Two identical cameras can be mounted via a beamsplitter to simultaneously acquire the FRET and CFP channels. In such an approach, image registration can be affected by camera orientation as well as the angle of the dichroic mirror (causing rotation, *x-y* translation, image shear, mismatched scale, and mismatched focus). One must carefully mount the cameras to minimize rotational and translational effects, while accounting for the focus differences. Typically, beamsplitters are designed with an adjustable parfocal compensation device that can independently adjust the focusing distance of either camera head. This should be performed empirically to minimize focus difference between the two channels. Rotation, *x-y* translation, shear, scaling difference, and curvatures in the field of view will need to be corrected computationally based on a priori calibration, as described in Basic Protocol 7.

EXPRESSION OF Rac1 FLAIR, DUAL-CHAIN FRET BIOSENSOR FOR Rac1

BASIC PROTOCOL 5

The Rac1 biosensor currently used by the authors of this unit is a modification of an older design, wherein the FRET donor was EGFP-Rac1 and the FRET acceptor was a small binding domain derived from p21-activated kinase 1 (PAK1), labeled with the dye Alexa 546 (Kraynov et al., 2000). We modified this biosensor by replacing the EGFP with the fluorescent protein CyPet, and replaced the Alexa 546 with the fluorescent protein YPet (Fig. 14.11.1C). The new Rac1-FLAIR biosensor is wholly genetically encoded. It has been extensively validated and compared with other designs (Machacek et al., 2009). Unlike the RhoA biosensor above, the donor and acceptor fluorophores are not on the same chain. This improves the dynamic range and hence the sensitivity of the biosensor (in single-chain designs, some residual FRET is usually present even in the off state, so the change induced by activation is not as great as in dual-chain designs). The disadvantage of the dual-chain design is that the two chains do not distribute equally through the cell, necessitating careful bleed-through correction (see Basic Protocol 7). The two designs are prone to different effects on cell physiology and artifacts affecting the activation signal. Controls for the Rac1 FLAIR biosensor indicate that results have not been compromised by the separation of the chains (Machacek et al., 2009), and the sensitivity is, in fact, substantially enhanced.

Expression of the Rac1 biosensor is essentially the same as described for the RhoA biosensor above. The Rac1 biosensor is available from Addgene (*http://www.addgene.org*) in two formats:

1. Mammalian expression and cloning vectors: pECFP-C1 (Clontech) with ECFP replaced by CyPet (pCyPet-Rac1/kanamycin resistance), and pEYFP-C1 (Clontech Inc.) with EYFP replaced by YPet (pYPet-PBD/kanamycin resistance).

2. pBabe-sin-tet-CMV-puro retroviral vector for Tet-On/Off system incorporating the CyPet-Rac1 and YPet-PBD (amp resistance).

Because the donor and acceptor chains are on separate expression constructs, co-transfection/transduction of both components is required.

Materials

Mouse embryo fibroblast (MEF/3T3) cells (Clontech; tet-OFF MEF/3T3)
Rac1 biosensor vector system (see above)
Fugene6 transfection reagent (Roche)
10 mg/ml doxycycline stock solution
Coverslips coated with fibronectin: immerse glass coverslips 30 to 60 min in 10 μg/ml fibronectin (e.g., Sigma), then rinse three times with PBS (*APPENDIX 2A*) and leave immersed in PBS until use

Additional reagents and equipment for cell culture techniques (*UNIT 1.1*), flow cytometric cell sorting (Robinson et al., 2009), and imaging the Rac1-FLAIR biosensor (Basic Protocol 6)

For transient expression

1a. Transfect mouse embryo fibroblast cells (MEF/3T3) using Fugene6 following the manufacturer's protocols. Use a DNA ratio of 3:2 to transfect CyPet-Rac1 and YPet-PBD, respectively, for optimal results in MEF (or COS-7) cells.

It is important to premix the DNA solutions in the correct ratio, then add them to the Fugene-containing medium as a single aliquot. This optimizes correct mixing of both DNA constructs and results in an evenly distributed expression profile 24 hr post-transfection.

2a. Plate cells on fibronectin-coated glass coverslips at a density of 4×10^4 cells/coverslip for 3 to 4 hr prior to imaging.

For stable cell lines

Stable cell lines are preferred to reduce variability in the fluorescence profile from experiment to experiment, as well as for attaining better control of expression levels.

1b. For viral transduction using the pBabe Tet-off system, cotransduce viruses for the donor and acceptor portions of the biosensor according to the manufacturer's instructions.

2b. Select cells for stable incorporation by successively increasing the puromycin concentration, similar to the procedure described for stable RhoA biosensor cells (see Basic Protocol 3, step 2).

3b. Once the stable population is produced, sort the cells flow cytometrically (Robinson et al., 2009) for low to medium brightness, with equal CyPet and YPet fluorescence emission,

4b. Replate the collected fraction with doxycycline (1 μg/ml) to repress the expression until 48 hr prior to experiments.

Examination of varying ratios and levels of expression for each construct have not affected the results of motility studies, but can influence sensitivity and the ease of bleed-through corrections.

BASIC PROTOCOL 6

IMAGING RAC1-FLAIR

Imaging is performed in Ham's F-12K medium without phenol red (see recipe in Reagents and Solutions), supplemented with 2% fetal bovine serum. For emission ratio imaging, the following filter sets (Chroma Technology) are used (for excitation and emission, respectively): CyPet: HQ436/20 (ex), HQ470/40 (em); FRET: HQ436/20 (ex), HQ535/30 (em); YPet: HQ500/20 (ex), HQ535/30 (em). The dichroic mirror ("Quad-Custom," lot no. 511112038; spectra shown in Fig. 14.11.4) was custom manufactured by Chroma

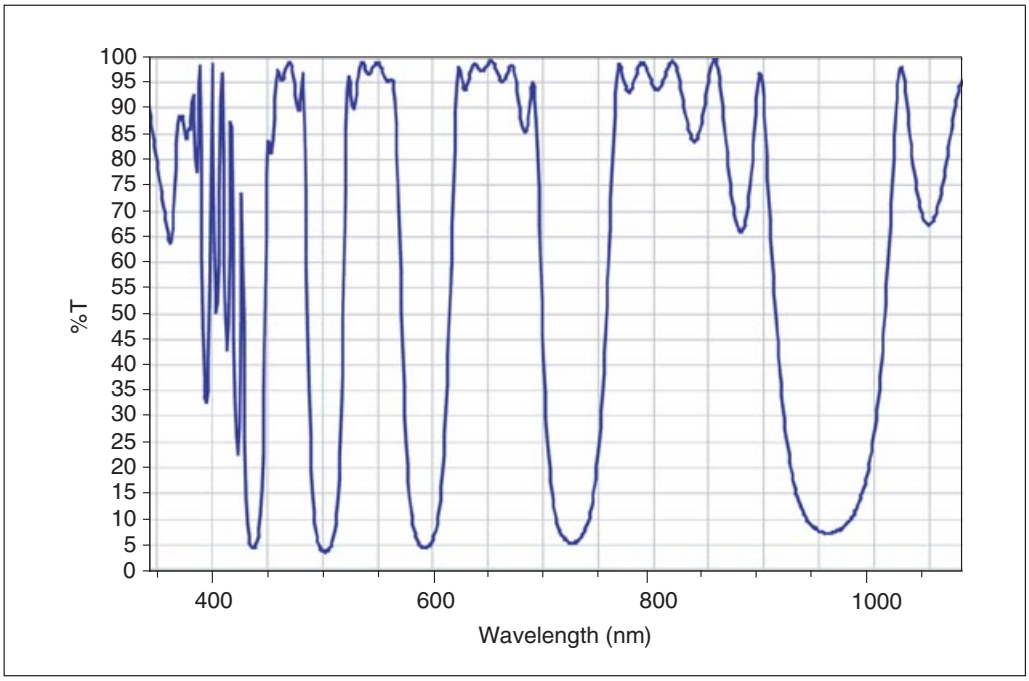

Figure 14.11.4 Transmittance spectra for the "Quad Custom" dichroic mirror (Chroma Technology, lot no. 511112038).

Technology Corp. for compatibility with all of these filter sets. A more recent sputter-coated ET series of dichroic mirrors and band-pass filters from Chroma could be used. For CyPet/YPet imaging or any other ECFP/EYFP-FRET-based imaging, either filter set 59217 (single-band exciters with a dual-band emitter) or set 89002 (all single-band filters) can be used effectively (Chroma Technology). Cells are illuminated with a 100 W Hg arc lamp through a neutral-density filter of 10% transmittance. At each time point, three images are recorded with the following exposure times, typical for the low biosensor concentrations used to minimize cell perturbation—CyPet, 900 msec; FRET (excitation of donor, observation of acceptor emission), 900 msec; YPet, 300 msec—at binning 2 × 2. The image sets have been taken at 10-sec to 10-min intervals. Ideally, one fills ~75% of the total 12-bit dynamic range of the camera for each channel. This produces a good signal-to-noise ratio and does not saturate the dynamic range should any one channel dramatically increase brightness. Imaging is detailed further in the RhoA biosensor section above.

Bleed-through correction for intermolecular biosensors is described in the following discussion of imaging procedures.

IMAGE PROCESSING PROCEDURES

BASIC PROTOCOL 7

Shading correction

The first step in image analysis is to correct for uneven illumination in the field of view. This is present in almost all images, including those taken using flat-field (Plan) corrected objective lenses. In order to correct for shading, one obtains images from fields of view that contain no samples. Images of each fluorescence channel are obtained using the same camera integration times and illumination conditions as are used for the real images that will be corrected. The images for shading correction are acquired following the acquisition of the real fluorescence image sets either by using cell-free areas within the same coverslip or by mounting a fresh coverslip with identical media and mounting conditions. In the latter case, it is convenient to mark a spot in the middle of the fresh coverslip on the side where cells would be present on an actual sample coverslip, so that one can focus on the edge of the spot to find the correct plane of focus. Usually, 20 to 30 shading images are acquired at the appropriate camera integration times and illumination settings for each fluorescence channel. The resulting image set for each channel is averaged to produce a single shade-corrected image for each fluorescence channel. The averaging process is important because each image frame contains stochastic camera noise. This noise can be reduced by averaging many frames of the same field of view. Additionally, images corrected for camera noise are required. These images are obtained by taking an average of multiple exposures (10 frames) of a field of view, but with the illumination shutter completely closed so as to prevent any light from reaching the CCD sensor. This basically captures the electronic and dark current noise associated with each acquisition condition. The noise image is then subtracted from the raw images and the shading images. Once these corrections are made, one simply divides the sample field of view by the corresponding shading image. Here, care must be taken to prevent floating-point errors from the image analysis software. Software including Metamorph (Universal Imaging Co.) and ISEE Inovision (ISee Imaging Systems) do not process floating-point data. Matlab (Mathworks) codes can be written to process images using a multiple decimal-point precision. Metamorph offers a convenient plug-in module for shade correction where a scaling factor can be specified to increase the relative pixel values so that floating-point operation is avoided. One can either scale to the maximum pixel value in the shading image or specify some fixed value. The latter is usually the better choice, as one can specify the same scaling factor (i.e., 1000) for images from both channels of fluorescence, thereby maintaining the relative intensities of the image pairs.

Background subtraction

Because of the flat-field correction, cell-free background areas within the field of view have the same intensities. One can use an area with minimal debris in the field of view as the background. The pixel intensities within such a region are averaged and subtracted from the whole image. Small variations in background can be introduced, e.g., by debris in your field of view. It is important to choose the same background position in each fluorescence image to minimize artifacts. Metamorph offers a convenient plug-in module ("Use region as background") to expedite the process. Using this utility, one can select a background region in the first fluorescence image of a ratio pair, and copy/save the region and paste/load onto the second fluorescence image. When using this Metamorph utility, it is important to note that processing of stack images requires additional considerations. If the region is selected on the top plane and the utility is run for all planes in the stack, the averaged background value from the first plane is subtracted from each of the subsequent planes. In order to work around this problem, the region on the top plane can be saved and loaded onto each of the subsequent planes, and background subtracted. Similarly, the same region can be loaded onto each plane of the fluorescence ratio pair images and processed.

Image masking

Ratio division can introduce noise and hot spots in regions outside of the cell. Furthermore, pixel intensities in the thin, peripheral regions of the cell can be near background levels, making reliable quantitative ratio calculations difficult. In order to limit the area within which ratio calculations are performed, a binary mask can be applied to the cell, setting areas outside of the cell uniformly to zero. The mask can be based on an image of a volume marker (i.e., fluorescent dextran) or a membrane marker in a fluorescence color different from that of the biosensor. This is used to unambiguously specify the true cell boundary in cases where intracellular distribution of the biosensor does not correspond to the cell shape. In the case of most GTPase biosensors, distribution of the biosensors sufficiently delineates the cell boundaries, so this is unnecessary.

To produce the binary mask, all fluorescence image stacks (dye and EGFP channels, or ECFP and FRET/Citrine-YFP channels) are intensity thresholded. If the shade correction and background subtraction have been performed correctly, this is a straightforward process (i.e., using the Threshold Image command in Metamorph). With properly processed images, the histogram distribution is such that there will be a large peak in the zero-pixel-intensity position, followed by a spread of non-zero pixels in the image histogram distribution (Fig. 14.11.5). Inclusive thresholding is manually performed by trial and error, observing which setting appropriately includes the cell pixels and excludes the surrounding pixels (i.e., using the Metamorph Threshold Image function). For a 16-bit image, the upper bound needs to be set at 65,535, the maximum value for 16-bit dynamic range. When processing a series of images from a time-lapse study, it is important to check the low-end threshold value selected using the first plane ($t = 0$ time point) against the last image plane ($t =$ end). Photobleaching will shift the low-end intensity distribution downward, resulting in under-selection of cell area at later times. In order to work around this problem, threshold values are determined through one of two methods: (1) thresholding is performed for later time points of the data stack, resulting in a relaxed thresholding for earlier time points; or (2) the data stack is histogram-equalized for the lowest intensity value using the Metamorph Equalize Light function, setting the equalization for "minimum" via the "addition" option, then producing the binary mask using the equalized data stack and then applying the resulting binary mask to the original non-equalized data stack. The latter approach produces better masking precision without resulting in relaxed selection in the earlier time points. Once the threshold values are set, a binary mask can be produced based on the selected inclusive threshold (in Metamorph, the Clip tab within the Threshold Image module is used to produce a binary mask in

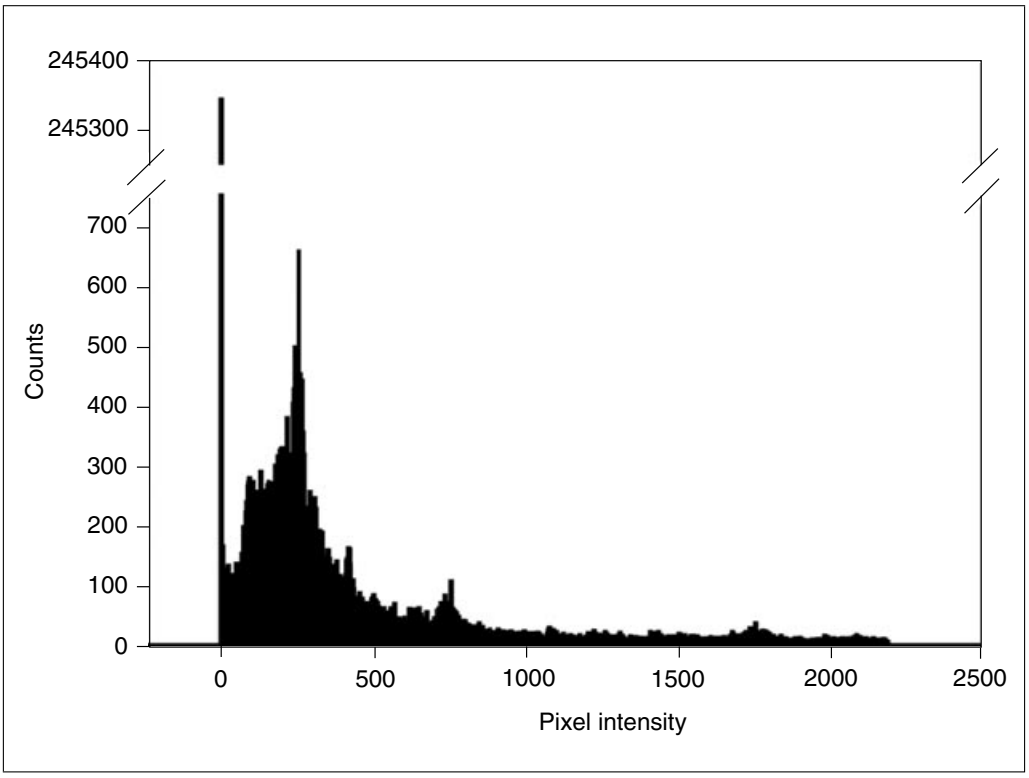

Figure 14.11.5 A representative histogram from a shade-corrected and background-subtracted image, prior to masking. The prominent histogram peak at zero intensity is followed by a continuous distribution of pixels at a range of positive intensity values. Threshold masking to remove pixels of too low an intensity is performed using this histogram. One maximizes selection of pixels from within the cell while removing pixels outside the cell, including noise around the periphery.

16-bit). This will produce a binary mask where regions outside the threshold selected area are uniformly zero, while inside is 65,535. Divide the binary mask with a constant (65,535) to produce a true binary mask containing the value one inside the masked region and zero outside (Arithmetic function in Metamorph). Binary masks produced for each fluorescence channel are multiplied into the corresponding fluorescence image stacks to produce the masked fluorescence image stacks prior to automated image registration.

Automated image registration

The ratio calculation requires a division of one image by another. It is essential that the fluorescence ratio image pair be perfectly aligned prior to division. There are a host of potential sources for misalignment: placement of optical filters, dichroic turret movement, *x-y-z* stage movement, temperature fluctuations and ambient vibration, and sub-pixel misalignment. Figure 14.11.3 indicates the result of misalignment on ratiometric analysis. The edge artifacts in the form of high ratio values on one side and low ratio values on the other, as well as similar symmetrical artifacts within the cell, provide clues that image misregistration has occurred. Sub-pixel registration routines are available in most image processing-software. For some experiments, only manual registration will suffice, but in many cases, especially when there are subcellular structures with clearly defined edges, automated registration is possible. The authors of this unit developed an automated method for image registration based on normalized cross-correlation technique (Shen and Price, 2006). A modified version of this routine, based on the Matlab program, applicable for registration of up to three channels of fluorescence image sets, is provided at *http;//www.currentprotocols.com/protocol/cb1411* (files `regAny2.m` and `regFCY2.m`).

The Matlab routine for processing the 2-channel data set is `regAny2.m` and for the 3-channel data set is `regFCY2.m`. The `regAny2.m` will take individual tiff files with the running number index and align the FRET channel with respect to the CFP channel to an accuracy of 1/20th of a pixel (maximum pixel shift allowed = 10 whole pixels). Similarly, the `regFCY2.m` will align the FRET and YFP channels against the CFP channel. In both cases, the relative displacements in *x* and *y* are recorded on a frame-by-frame basis for an entire time series, and the median values of the distance displacements in *x* and *y* are applied to the whole time series at the end of the routine. This mode of registration is based on the assumption that the majority of the channel misalignment will stay constant for the duration of a single time-lapse experiment. If individual *x-y* displacements are corrected on a frame-by-frame basis, we have observed an unacceptable level of jitter in the final movie playback. Detailed requirements for the naming convention, file formats, etc., are listed within the headers of the programs. One tip for making this program run faster and more smoothly is to crop the cell image as tightly as possible (ensuring for all timepoints that the cell stays within the region of interest selected and cropped), making sure both channels to be aligned are cropped using the same cropping factor. This will minimize the computational load required to translationally align the images, as there will be fewer total pixels to compute the cross-correlation coefficients compared to processing the entire field of view.

Image shear, rotation, and scaling correction

Two separate cameras can be used to simultaneously acquire the two images required for ratio imaging (CFP and FRET, or EGFP and dye). This can be valuable when rapid image sequences are required, or when rapid changes in cell shape or biosensor distribution can produce motion artifacts. For simultaneous imaging with two cameras, one uses a beam splitter and appropriate filters and dichroic mirror to direct different wavelengths to each camera. Differences in positioning of the two cameras can produce image misalignment other than the straightforward *x-y* translation encountered with one camera. Such additional misalignments include shear, rotation, and scaling between the two images. These problems primarily arise from imperfect mounting of the cameras and the dichroic mirrors in the beam splitter. Alignment should first be optimized manually, but an automated solution based on a priori calibration is required to sufficiently correct these effects. We present here a polynomial-based method for a priori calibration. Figure 14.11.6 shows calibration grid images and ratiometric images of RhoA activity before and after the correction. It is clear that manually aligning one corner of the grid leads to misalignment of the far corner. The software for Matlab consists of two parts (*http://cuurrentprotocols.com/protocol/cb1411*, files `morphPrep.m` and `morph.m`): (1) a priori calibration software `morphPrep.m`, used to determine the coordinate transformation control points; and (2) the transformation program `morph.m`, which applies a 3rd-order polynomial-based coordinate transformation using the calibrated control points. We find it best to apply these corrections prior to image masking and *x-y* translational alignment. For calibration, one can use a grid-type stage micrometer imaged in bright-field, or microbeads coated with fluorophores to simulate fluorescence imaging conditions. Imaging of the calibration specimen should be performed at the end of an experiment (be careful not to move the two cameras during the imaging experiment!). This correction method is not applicable to a majority of cases where a single camera and filter wheel are used to acquire multiple images in succession. However, in some cases fluorophores of very different wavelengths can scale differently due to the behavior of chromatically corrected optics (i.e., ECFP versus Cy-7). This method can be used effectively to correct for such issues if a priori calibration is performed.

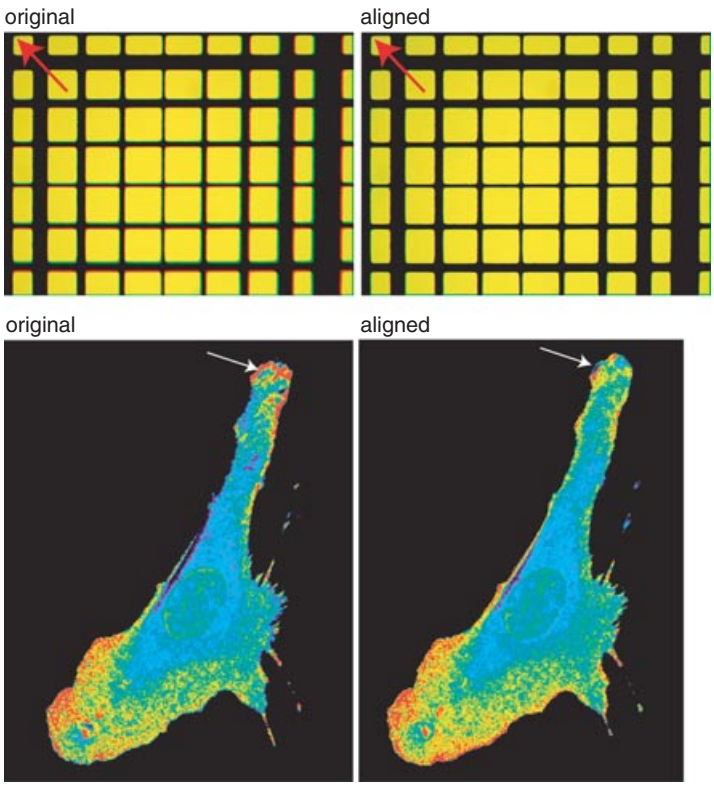

Figure 14.11.6 Image shear between two cameras creates artifacts in ratio images. In the upper panels, calibration grid images from two cameras are overlaid with and without shear correction (red arrow: two channels aligned relative to the corner indicated). In the lower panels, the ratios of RhoA biosensor readouts from the two camera channels are shown with and without shear correction. A peripheral ruffle shows a large artifactual feature when correction is not applied (white arrow). For color figure go to *http://www.currentprotocols.com/protocol/cb1411*.

Ratio calculation

The masked and registered images are divided to produce a ratio image. For meroCBD, the dye image is divided by the EGFP image. For the FRET sensors, the FRET channel is divided by the donor image. The floating point error consideration is important in this step; for software that does not carry out floating point calculations, all numbers must be multiplied by a constant. This converts decimal portions of intensity values to larger numbers, so that they are not truncated or otherwise modified prior to division. In the Metamorph Arithmetic module, a scaling factor of 1000 is specified as a multiplication factor during the ratio calculation. A smaller factor (10 to 100) can be used. However, this is not recommended since it tends to produce a non-smooth histogram distribution (Fig. 14.11.7). The same scaling factor should be used when comparing ratio calculations from different experiments with the same biosensor.

Ratio images are scaled and often displayed as a pseudocolor map to reflect the range of ratio values within the image. Many methods are used for this, and the range of values within an image cannot readily be used to determine the dynamic range of the biosensor. For example, the lowest and highest pixel intensities are often not included in the scaling, as these can be due to spurious artifacts or noise. If one chooses to eliminate the lowest and highest 1% of pixel intensities, a 99-fold change is shown within the image. Eliminating the lowest and highest 5% reduces this to a 20-fold change.

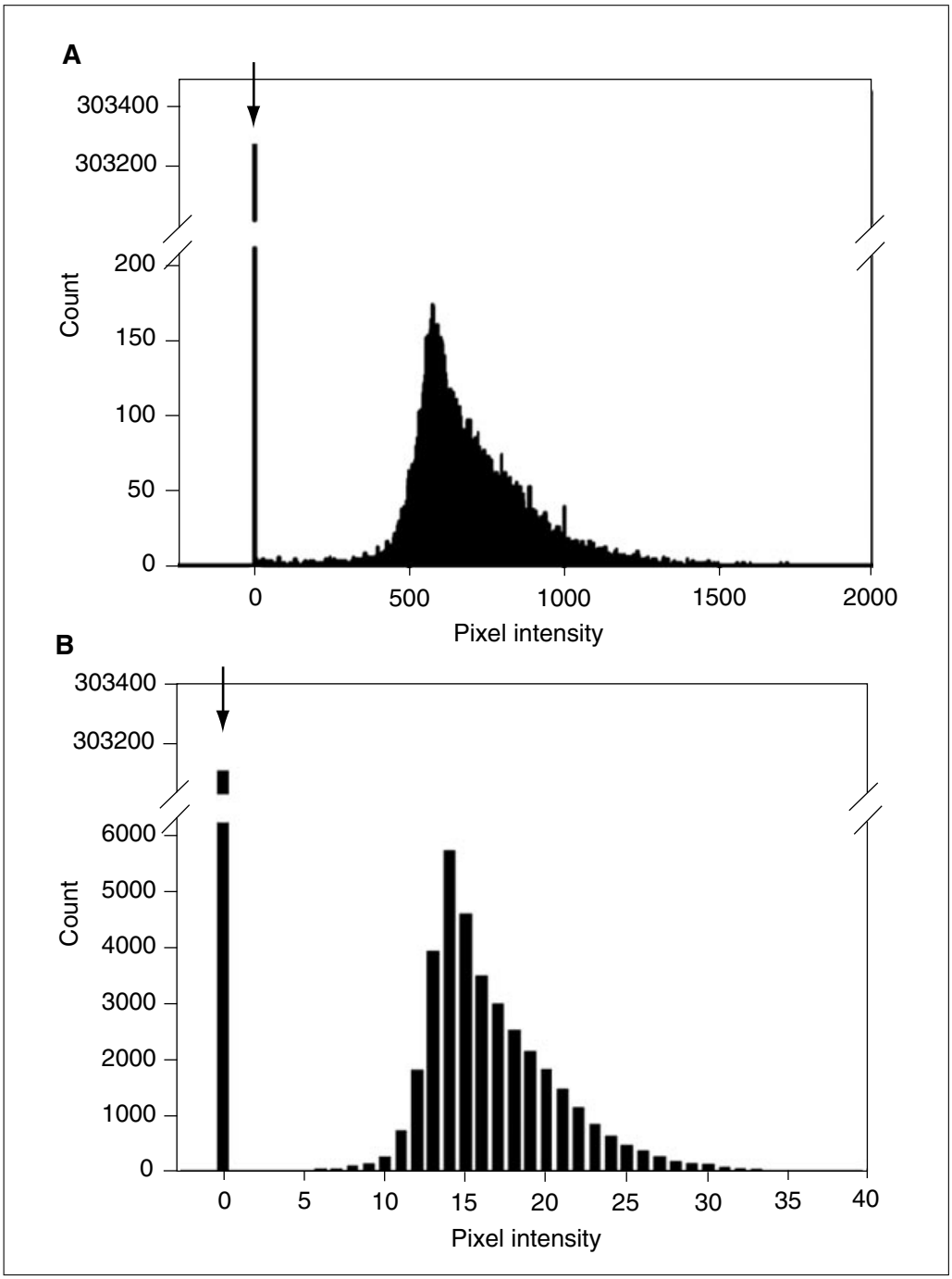

Figure 14.11.7 Effect of the multiplication factor during ratiometric calculation. In panel (**A**), using a scaling factor of 1000 produced a smooth histogram distribution in a ratio image. Panel (**B**) shows the same ratio image with the scaling factor of 25. Though the general distribution pattern is similar, the histogram distribution in (A) retains higher bit-depth resolution.

Ratio calculations for intermolecular FRET biosensors

In the case of intermolecular FRET biosensors such as the biosensor for Rac1, a bleed-through correction is required. Images for the bleed-through correction should be obtained routinely as part of each experiment, so that variations in the microscope system over time do not come into play. Control cells expressing either CyPet alone or YPet alone are used to determine how much light bleeds through into channels where it is not desirable. For example, CyPet excitation is used to generate FRET. However, when this is done, some light emitted from CyPet itself appears in the FRET emission channel.

This bleed-through must be quantified so that it can be subtracted out in real experiments. For this correction, intensity is measured using the CyPet excitation and CyPet emission channels, then measured again under the same exposure conditions using the CyPet excitation and YPet emission channels that will be used to monitor FRET. This reveals what percentage of the intensity measured using the direct CyPet fluorescence channels would also appear in the FRET channels. Bleed-through coefficients determined in this way are the coefficients α and β in the following equation:

$$R = \frac{\mathrm{FRET_t} - (\alpha \times \mathrm{CyPet}) - (\beta \times \mathrm{YPet})}{\mathrm{CyPet}}$$

Equation 14.11.3

where R is the ratio, $\mathrm{FRET_t}$ is the total FRET intensity as measured, α is the bleed-through of CyPet into FRET channel upon CyPet excitation, β is the bleed-through of YPet into FRET channel upon CyPet excitation of YPet, and CyPet is the total CyPet intensity as measured. Bleed-through into the CyPet channel (denominator) is negligibly small. By calculating the linear slope of the relationship between FRET and CyPet intensities upon CyPet excitation of cells expressing only the CyPet, the bleed-through parameter α can be determined. Similarly, by relating bleed-through into the FRET channel upon CyPet excitation of cells expressing only the YPet, the bleed-through contribution of YPet excitation by CyPet excitation into the FRET channel β can be determined. For our microscope and exposure conditions, the α parameter was found to be routinely within 0.4 and 0.5 and the β parameter to be $\sim$0.2. These are dependent on the optical configuration of the microscope used. We provide a convenient Matlab routine, `BT_AB.m` for calculating the α and β parameters from raw images and associated shading images (*http://www.currentprotocols.com/protocol/cb1411*; file `BT_AB.m`), utilizing a segmentation based on the K-means clusters method (Shen and Price, 2006). The ratio of corrected FRET over CyPet can be calculated and used as a measure of Rac1 activation.

In time-lapse experiments, CyPet and YPet photobleach at different rates. The ratio can be corrected for photobleaching as described elsewhere (Hodgson et al., 2006). Briefly, by algebraic manipulation, Equation 14.11.3 can be rearranged to:

$$R = \frac{\mathrm{FRET_t}}{\mathrm{CyPet}} - \beta \frac{\mathrm{Ypet}}{\mathrm{CyPet}} - \alpha = \Gamma - \beta \times \Psi - \alpha$$

Equation 14.11.4

where Γ is the fraction representing total FRET intensity over total CyPet intensity, and Ψ is the fraction representing total YPet intensity over total CyPet intensity, and both α and β are bleed-through constants described before. By taking double exponential fits of the decays of both Γ and Ψ, the correction function, $\bar{R}^{-1}$, can be calculated as outlined previously (Hodgson et al., 2006). We provide a convenient routine, `PB5.m`, that takes the masked and registered image sets (CyPet, YPet, and FRET) plus the a priori–determined α and β parameters, and calculates the photobleach-corrected ratio R and corrected FRET, which is represented by the numerator of Equation 14.11.3 (see *http://www.currentprotocols.com/protocol/cb1411*; file `PB5.m`). These codes are available for download from the Hahn lab Web page and from the Current Protocols Web site (*http://www.currentprotocols.com/cb1411*). Also included are the Matlab routines `SubpixShift.m`, `subalign.m`, `kmeanst.m`, and `maxArray.m`,which are required functions that are called from within the routines described above.

REAGENTS AND SOLUTIONS

Use deionized, distilled water in all recipes and protocol steps. For common stock solutions, see ***APPENDIX 2A****; for suppliers, see* ***SUPPLIERS APPENDIX****.*

Ham's F-12K, phenol red-free

Inorganic salts
7530.00 mg/liter NaCl
285 mg/liter KCl
106 mg/liter $MgCl_2 \cdot 6H_2O$
393 mg/liter $MgSO_4 \cdot 7H_2O$
135 mg/liter $CaCl_2$
218 mg/liter $Na_2HPO_4 \cdot 7H_2O$
59 mg/liter KH_2PO_4
2500.00 mg/liter $NaHCO_3$
0.8 mg/liter FeSO4·$7H_2O$
2 μg/liter $CuSO_4 \cdot 5H_2O$
0.14 mg/liter $ZnSO_4 \cdot 7H_2O$

Amino acids
17.8 mg/liter L-alanine
421.3 mg/liter L-arginine HCl
30 mg/liter L-asparagine·H_2O
26.6 mg/liter L-aspartic acid
70.04 mg/liter L-cysteine HCl·H_2O
0 mg/liter L-cystine
29.4 mg/liter L-glutamic acid
15 mg/liter glycine
41.9 mg/liter L-histidine HCl·H_2O
7.9 mg/liter L-isoleucine
26.2 mg/liter L-leucine
73.1 mg/liter L-lysine HCl
8.9 mg/liter L-methionine
9.9 mg/liter L-phenylalanine
69.1 mg/liter l-proline
21 mg/liter L-serine
23.8 mg/liter L-threonine
4.1 mg/liter L-tryptophan
10.9 mg/liter L-tyrosine
23.4 mg/liter L-valine

Vitamins
0 mg/ml L-ascorbic acid
0.07 mg/ml biotin
0.48 mg/ml D-calcium pantothenate
13.96 mg/liter choline chloride
1.36 mg/liter cyanocobalamin
1.32 mg/liter folic acid
18 mg/liter inositol
0.04 mg/liter nicotinamide
0.06 mg/liter pyridoxine HCl
0.04 mg/liter riboflavin
0.21 mg/liter thiamine HCl
0.21 mg/liter DL-thioctic acid

continued

Other compounds
1260.00 mg/liter glucose
0 mg/liter linoleic acid
4 mg/liter hypoxanthine·Na
0 mg/liter phenol red
0.3 mg/liter putrescine
220 mg/liter sodium pyruvate
0.7 mg/liter thymidine

Lysis buffer

50 mM sodium phosphate buffer, pH 7.6 (*APPENDIX 2A*)
300 mM NaCl
10% (w/v) glycerol
5 mM $MgCl_2$
2 mM 2-mercaptoethanol (omit where indicated in protocol)
1 mM PMSF (omit where indicated in protocol)
Store up to 12 months at 4°C

Storage buffer

50 mM Tris·Cl, pH 7.5 (*APPENDIX 2A*)
50 mM NaCl
5 mM $MgCl_2$
10% (w/v) glycerol
Store up to 12 months at 4°C

COMMENTARY

Background Information

Biosensors have become valued tools in cell biology, with commercial software and specifically designed microscopes greatly enhancing their accessibility and ease of use. It is important to apply this software with an understanding of the variables that can affect biological conclusions. Final images are sensitive to subtle changes in image-processing procedures, or the use of biosensors under conditions that affect cell biology. The authors of this unit hope that the procedures outlined here, for three different biosensor designs, can be a guide for proper application of new biosensors to shed light on previously invisible protein dynamics.

Rac1 FLAIR is an intermolecular FRET biosensor, frequently referred to as a dual-chain sensor. The use of a dual-chain design significantly enhances the sensitivity of the biosensor in comparison with single-chain FRET biosensors. The latter usually show substantial FRET even when the biosensor is in the off state; the two fluorophores are never fully separated. With the Rac1 sensor, the dynamic range, the difference between the on and off states, is enhanced. There is a downside to the dual-chain approach. The two components of the biosensor distribute differently in the cell, necessitating additional steps in image processing. Both single-chain and dual-chain biosensors are potentially perturbed by competition from native protein ligands; the dual-chain sensor may be more likely to produce false negatives, as it may be more sensitive to ligands that compete for the GTPase-binding fragment, while the steric bulk of the single-chain sensor may prevent it from reaching all sites normally accessed by the GTPases. The issue of competition and its effect on biosensor readout is complex and beyond the scope of this unit. We recently completed a careful study of the effects of varying the concentration of each component of the dual-chain Rac1 biosensor. This did not appreciably alter the results of our cell protrusion studies (Machacek et al., 2009).

Factors affecting FRET efficiency

FRET is sensitive to both the distance and orientation of the two fluorophores in a biosensor. When fluorophores are sufficiently far apart or have orthogonal dipole orientations, excitation of the donor leads simply to donor emission, rather than to FRET. However, when the distance is sufficiently small, and orientation enables sufficient dipole coupling, excitation energy is transferred from the donor

to the acceptor, leading to decreased donor emission and increased emission from the acceptor. This produces a characteristic FRET excitation/emission spectrum, different from that of the donor or the acceptor alone.

GFP mutants optimized for FRET in living cells have shown impressive improvements. Mutants incorporate different trade-offs between brightness, FRET efficiency, photostability, and pH dependence of fluorescence characteristics (Heikal et al., 2000; Miyawaki and Tsien, 2000). Enhanced brightness improves the overall signal-to-noise ratio in cells, but is not always an improvement if it comes at the cost of FRET efficiency or photostability (Nguyen and Daugherty, 2005). The Cyan and Yellow fluorescent proteins (CFP and YFP), and their brighter, pH-stable versions Cerulean and Venus (Miyawaki and Tsien, 2000; Rizzo and Piston, 2005), are relatively fast-maturing, bright GFP mutants that have proven useful in many FRET biosensors. More recent mutants with improved FRET efficiency (Nguyen and Daugherty, 2005) include CyPet and YPet, which exhibit 6- to 7-fold greater FRET efficiency than the original CFP-YFP pair, though more recent findings indicated that this particular pair may be more prone to dimerization (Nguyen and Daugherty, 2005; Ohashi et al., 2007).

FRET efficiency is quantified by the Förster equation:

$$R_0 = \left[8.8\times10^{23} K^2 n^{14} Q_d J\right]^{1/6}$$

Equation 14.11.5

where R_o is the Förster distance (distance at which energy transfer is 50% efficient) and K^2 is the dipole orientation factor, a function of the donor emission transition moment and the acceptor absorption transition moment. K^2 = 2/3 is generally assumed when fluorophore rotation can occur about the bond attaching the fluorophore to the protein (Lakowicz, 1999). Q_d is the fluorescence quantum yield of the donor in the absence of acceptor, n is the refractive index of the medium, generally assumed to be 1.4 for proteins (dos Remedios and Moens, 1995), and J is the spectral overlap integral, indicating the extent of overlap between the donor fluorescence emission spectrum and the acceptor excitation spectrum (Lakowicz, 1999).

In FRET biosensors, activation of the targeted protein leads to a change in the distance and/or orientation of the fluorophores. FRET efficiency is exquisitely sensitive to distance between fluorophores (varies as the inverse 6th power of the distance between the fluorophores):

$$E = \frac{R_0^6}{\left(R_0^6 + R^6\right)}$$

Equation 14.11.6

where E is FRET efficiency, R_o is the Förster distance, and R is the actual distance (Lakowicz, 1999). Changes in the relative angular orientations of the dipoles produce a lesser but nonetheless important effect; the dipole orientation factor K^2 can be assumed to be 2/3 only when both fluorophores are free to rotate isotropically during the excited-state lifetime. A change in the fixed angle of the fluorophores in different biosensor states affect FRET because K^2 can change between 0 and 4 (Lakowicz, 1999; dos Remedios and Moens, 1995). The effects of fluorophore separation (linear displacement) versus angular reorientation cannot be readily separated in live-cell studies, so FRET changes are not used to precisely determine distances between proteins in cells. Rather, the extent of FRET produced by fully activated versus inactive target protein is determined, and these endpoints are used to interpret FRET signals in vivo.

Critical Parameters and Troubleshooting

The critical parameters for setting up a microscope system for time-lapse biosensor imaging will not be discussed here, as the relevant protocols above deal with these in detail. For successful biosensor imaging, critical components are production of clean and functional biosensor at optimal dye labeling efficiency in the case of meroCBD, and optimal expression levels and cell health in the case of genetically encoded biosensors. The proper maintenance of cells before and after microinjection will significantly affect cell survival during time-lapse imaging in the case of MeroCBD. We have found that careful attention to deoxygenating the imaging medium, using reagents including Oxyrase/Oxyfluor, has a significant effect in minimizing photobleaching as well as photodamage to cells from irradiation. To this end, use of low-intensity light for a longer duration of exposure is much preferred, rather than a short exposure with a full intensity of excitation light.

The choice of imaging medium is an important consideration when imaging FRET biosensors. Background fluorescence from the

medium is a significant issue at the wavelengths used. We have performed a quantitative comparison of various media available commercially (data not shown), and concluded that Ham's F-12K medium without phenol red (Kaighn, 1973; Robey and Termine, 1985; see Reagents and Solutions) is a good choice. Unfortunately, this medium is no longer commercially available. The published formulation can be found in Reagents and Solutions.

Anticipated Results

Biosensors for Rho family GTPases should provide sensitive and high-resolution data of activation of GTPases in living cells. Typically, only 40% to 60% of the CBD-EGFP is recovered as purified meroCBD, due to some denaturation/precipitation during labeling and loss during gel filtration. The final eluate concentration is usually 120 to 140 μM. Labeling efficiency under these conditions varies between a dye/protein ratio of 0.7 and 0.9. The meroCBD solution is divided into 15- to 20-μl aliquots and stored at –80°C. Flash-freezing using liquid N_2 or dry ice appears to increase precipitation during microinjection. Alternatively, meroCBD may be kept at 4°C for up to 1 week.

The single-chain RhoA and bimolecular Rac1 biosensor transduction using retrovirus usually results in a nearly 100% positive population following FACS sorting. FACS sorting with relatively tight gates is used to isolate a low-expression-level population that results in biosensor expression levels of ~20% to 30% of endogenous protein. For microscopy imaging, the typical time resolution can be in the order of seconds, limited only by the user's microscope system configuration. The spatial resolution can be theoretically at the optical limit of light microscopy in *x* and *y*; however, due to low levels of injection/expression that are preferred so as to not impact the biological processes of interest, binning may be required to increase sensitivity. The 2 × 2 binned dataset obtained using a 40× DIC oil-immersion objective lens will be on the order of 320-nm spatial resolution in *x* and *y*. The dynamic range of the biosensor ratio readout for meroCBD can be on the order of 1:3 to 1:6, that of genetically encoded single-chain RhoA biosensor can be on the order of 1:1.5 to 1:2, and that of genetically encoded bimolecular Rac1 biosensor can be on the order of 1:7 to 1:20. Dynamics of the resulting ratio readouts should be carefully interpreted, keeping in mind the potential sources of artifacts, including misalignment of the ratio pair and motion artifacts if using single camera-based imaging approach. These artifacts will significantly skew the resulting ratio and impact spatial as well as temporal ratiometric readouts.

Time Considerations

Preparation of meroCBD requires 3 days, including the dye-labeling reaction and post-reaction purification. Cells plated on fibronectin-coated coverslips are usually ready for microinjection within 3 hr following plating. Microinjection of live cells on coverslips is typically performed within 10 min, followed by a 30-min to 1-hr recovery prior to imaging experiments. The process of viral transduction can be performed, taking 1 week, while preparation of stable cell lines containing the genetically encoded biosensor can take up to 2 weeks, including the FACS sorting. Genetically encoded biosensors will require 48 hr after removal of doxycycline from the medium to induce expression prior to imaging experiments. Imaging experiments using the biosensors can be as long as the biological process of interest, but are usually limited to ~2 hr for meroCBD experiments, and can be extended to overnight for genetically encoded biosensors. The post-imaging data processing will require ~10 min per data set.

Literature Cited

Ausubel, F.M., Brent, R., Kingston, R.E., Moore, D.D., Seidman, J.G., Smith, J.A., and Struhl, K. (eds.). 2009. Current Protocols in Molecular Biology. John Wiley & Sons, Hoboken, N.J.

Del Pozo, M.A., Klosses, W.B., Alderson, N.B., Meller, N., Hahn, K.M., and Schwartz, M.A. 2002. Integrins regulate GTP-Rac localized effector interactions through dissociation of Rho-GDI. *Nat. Cell Biol.* 4:232-239.

dos Remedios, C.G. and Moens, P.D. 1995. Fluorescence resonance energy transfer spectroscopy is a reliable "ruler" for measuring structural changes in proteins: Dispelling the problem of the unknown orientation factor. *J. Struct. Biol.* 115:175-185.

Heikal, A.A., Hess, S.T., Baird, G.S., Tsien, R.Y., and Webb, W.W. 2000. Molecular spectroscopy and dynamics of intrinsically fluorescent proteins: Coral red (dsRed) and yellow (Citrine). *Proc. Natl. Acad. Sci. U.S.A.* 97:11996-12001.

Hodgson, L., Nalbant, P., Shen, F., and Hahn, K. 2006. Imaging and photobleach correction of Mero-CBD, sensor of endogenous Cdc42 activation. *Methods Enzymol.* 406:140-156.

Kaighn, M.E. 1973. Tissue Culture Methods and Applications (J. Kruse and J. Patterson, eds.) Academy Press, New York.

Kraynov, V.S., Chamberlain, C., Bokoch, G.M., Schwartz, M.A., Slabaugh, S., and Hahn, K.M. 2000. Localized Rac activation dynamics visualized in living cells. *Science* 290:333-337.

Lakowicz, J.R. (ed.). 1999. Principles of Fluorescence Spectroscopy, pp. 368-377. Kluwer Academic/Plenum Publishers, New York.

Machacek, M., Hodgson, L., Welch, C., Elliott, H., Pertz, O., Nalbant, P., Abell, A., Johnson, G.L., Hahn, K.M., and Danuser, G. 2009. Coordination of Rho GTPase activities during cell protrusion. *Nature* 461:99-103.

Michaelson, D., Silletti, J., Murphy, G., D'Eustachio, P., Rush, M., and Phillips, M.R. 2001. Differential localization of Rho GTPases in live cells: Regulation by hypervariable regions and RhoGDI binding. *J. Cell Biol.* 152:111-126.

Miyawaki, A. and Tsien, R.Y. 2000. Monitoring protein conformations and interactions by fluorescence resonance energy transfer between mutants of green fluorescent protein. *Methods Enzymol.* 327:472-500.

Nalbant, P., Hodgson, L., Kraynov, V., Toutchkine, A., and Hahn, K.M. 2004. Activation of endogenous Cdc42 visualized in living cells. *Science* 305:1615-1619.

Nguyen, A.W. and Daugherty, P.S. 2005. Evolutionary optimization of fluorescent proteins for intracellular FRET. *Nat. Biotechnol.* 23:355-360.

Ohashi, T., Galiacy, S.D., Briscoe, G.M., and Erickson, H.P. 2007. An experimental study of GFP-based FRET, with application to intrinsically unstructured proteins. *Protein Sci.* 16:1429-1438.

Pertz, O., Hodgson, L., Klemke, R.L., and Hahn, K.M. 2006. Spatiotemporal dynamics of RhoA activity in migrating cells. *Nature* 440:1069-1072.

Rizzo, M.A. and Piston, D.W. 2005. A high contrast method for imaging FRET between fluorescent proteins. *Biophys. J.* 88:L14-L16.

Robey, P.G. and Termine, J.D. 1985. Human bone cells in vitro. *Calcif. Tissue Int.* 37:453-460.

Robinson, J.P., Darzynkiewicz, Z., Hoffman, R., Nolan, J.P., Orfao, A., Rabinovitch, P.S., and Watkins, S. (eds.). 2009. Current Protocols in Cytometry. John Wiley & Sons. Hoboken, N.J.

Sambrook, J., Fritsch, E.F., and Maniatis, T. 1989. Molecular Cloning: A Laboratory Manual. Cold Spring Harbor Laboratory Press, Cold Spring Harbor, N.Y.

Shen, F. and Price, J.H. 2006. Melanoma coculture outgrowth model for testing complete tumor contaminant ablation. *Cytometry A* 69:573-581

Shen, F., Hodgson, L., and Hahn, K. 2006. Digital autofocus methods for automated microscopy. *Methods Enzymol.* 414:620-632.

Shen, F., Hodgson, L., Price, J.H., and Hahn, K.M. 2008. Digital differential interference contrast autofocus for high-resolution oil-immersion microscopy. *Cytometry A* 73:656-666.

Toutchkine, A., Kraynov, V., and Hahn, K. 2003. Solvent-sensitive dyes to report protein conformational changes in living cells. *J. Amer. Chem. Soc.* 125:4132-4145.

Toutchkine, A., Nguyen, D.V., and Hahn, K.M. 2007a. Simple one-pot preparation of water-soluble, cysteine-reactive cyanine and merocyanine dyes for biological imaging. *Bioconjug. Chem.* 18:1344-1348.

Toutchkine, A., Nguyen, D.V., and Hahn, K.M. 2007b. Merocyanine dyes with improved photostability. *Org. Lett.* 9:2775-2777.

Wang, Y.L. 2007a. Computational restoration of fluorescence images: Noise reduction, deconvolution, and pattern recognition. *Methods Cell Biol.* 81:435-445.

Wang, Y.L. 2007b. Noise-induced systematic errors in ratio imaging: Serious artifacts and correction with multi-resolution denoising. *J. Microsc.* 228:123-131.